JOURNAL OF GEOPHYSICAL RESEARCH, VOL. 113, G01023, doi:10.1029/2007JG000435, 2008

An estimate of monthly global emissions of anthropogenic CO_2: Impact on the seasonal cycle of atmospheric CO_2

D. J. Erickson III,[1,2] R. T. Mills,[1] J. Gregg,[3] T. J. Blasing,[4] F. M. Hoffman,[1] R. J. Andres,[4] M. Devries,[1,5] Z. Zhu,[6] and S. R. Kawa[6]

Received 27 February 2007; revised 10 October 2007; accepted 4 December 2007; published 15 March 2008.

[1] Monthly estimates of the global emissions of anthropogenic CO_2 are presented. Approximating the seasonal CO_2 emission cycle using a 2-harmonic Fourier series with coefficients as a function of latitude, the annual fluxes are decomposed into monthly flux estimates based on data for the United States and applied globally. These monthly anthropogenic CO_2 flux estimates are then used to model atmospheric CO_2 concentrations using meteorological fields from the NASA GEOS-4 data assimilation system. We find that the use of monthly resolved fluxes makes a significant difference in the seasonal cycle of atmospheric CO_2 in and near those regions where anthropogenic CO_2 is released to the atmosphere. Local variations of 2–6 ppmv CO_2 in the seasonal cycle amplitude are simulated; larger variations would be expected if smaller source-receptor distances could be more precisely specified using a more refined spatial resolution. We also find that in the midlatitudes near the sources, synoptic scale atmospheric circulations are important in the winter and that boundary layer venting and diurnal rectifier effects are more important in the summer. These findings have implications for inverse-modeling efforts that attempt to estimate surface source/sink regions especially when the surface sinks are colocated with regions of strong anthropogenic CO_2 emissions.

Citation: Erickson, D. J., III, R. T. Mills, J. Gregg, T. J. Blasing, F. M. Hoffman, R. J. Andres, M. Devries, Z. Zhu, and S. R. Kawa (2008), An estimate of monthly global emissions of anthropogenic CO_2: Impact on the seasonal cycle of atmospheric CO_2, *J. Geophys. Res.*, *113*, G01023, doi:10.1029/2007JG000435.

1. Introduction

[2] The anthropogenic source of CO_2 to the atmosphere is an important term in the global carbon budget [*Marland and Rotty*, 1984; *Andres et al.*, 1996; *Bousquet et al.*, 2000; *Gurney et al.*, 2004]. Determining the relative contributions of the various sources and sinks of atmospheric CO_2 in different regions is critical to understand the global carbon budget [*Fan et al.*, 1998; *Denning et al.*, 1995; *Kaminski et al.*, 1999; *Randerson et al.*, 1997; *Engelen et al.*, 2002]. The anthropogenic CO_2 source is derived from a number of different processes including combustion of coal, oil, and natural gas, as well as oxidation of organic solvents and cement manufacture [*U.S. EPA*, 2006]. The majority of global estimates of anthropogenic CO_2 fluxes to the atmosphere have been compiled or modeled on an annual basis [*Marland and Rotty*, 1984; *Marland et al.*, 2006; *U.S. EPA*, 2006]. Here we use a 2-harmonic Fourier series approximation to impose a seasonal cycle on the annual fluxes and examine the impact of these monthly anthropogenic surface CO_2 fluxes on atmospheric CO_2 concentrations using a 3-D atmospheric transport model driven by assimilated winds [*Kawa et al.*, 2004].

2. Methods

[3] We experimented with a variety of methods that transform the annual mean CO_2 fluxes to monthly values by using national annual totals by fuel type. *Blasing et al.* [2005] presented monthly fossil-fuel carbon emissions in the United States (U.S.) from 1981 through 2002 derived from monthly energy consumption data at the national level provided by the Energy Information Agency. Their results show a clear and repetitive peak for total carbon emissions in the winter months and a growing secondary peak during the summer months. When broken down by fuel type, it is seen that consumption of natural gas is primarily responsible for the winter peak, and coal consumption produces smaller peaks during summer and winter. Combustion of liquid fuels produces more carbon emissions than natural gas or coal, but the annual pattern of emissions from liquid fuels is flat. Figure 1 shows average fossil-fuel carbon

[1]Computational Earth Sciences Group, Computer Science and Mathematics Division, Oak Ridge National Laboratory, Oak Ridge, Tennessee, USA.
[2]Nicholas School of the Environment and Earth Sciences, Duke University, Durham, North Carolina, USA.
[3]Geography Department, University of Maryland, College Park, Maryland, USA.
[4]Environmental Sciences Division, Oak Ridge National Laboratory, Oak Ridge, Tennessee, USA.
[5]School of Engineering, Vanderbilt University, Nashville, Tennessee, USA.
[6]Laboratory for Atmospheres, NASA Goddard Space Flight Center, Greenbelt, Maryland, USA.

0148-0227/08/2007JG000435$09.00

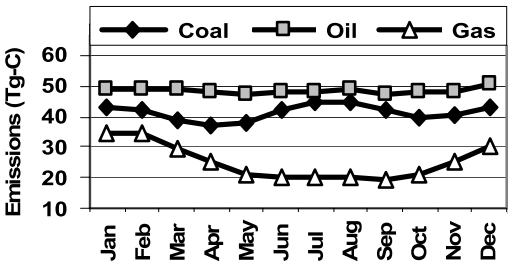

Figure 1. Five-year (2000–2004) averages of monthly fossil-fuel carbon emissions from combustion of coal, petroleum products (oil) and natural gas in the United States.

emissions for each calendar month for each fuel type averaged over the period 2000–2004, scaled so that each month represents an equal number of days. These data represent an update of the material presented by *Blasing et al.* [2005], based on fuel data provided by the Energy Information Administration of the U.S. Department of Energy.

[4] Heating demand follows a cosine curve over the course of the year. In the United States this is represented by natural gas which is the primary fuel used for space heating. So the usage and the CO_2 fluxes naturally peak in the winter and are minimal in the summer. Emissions from coal burning have two peaks, one in the summer and one in the winter. Electricity demand for lighting and indoor activities is also high during winter, but another peak associated with air conditioning demand appears in summer. Over 90% of the coal produced in the United States is used by the electric power sector [*EIA*, 2006], so the electricity-demand curve is similar to fossil-fuel emissions from coal combustion, and appears as a second harmonic. It should be noted that emissions from liquid fuels have a very small seasonality. These functions can be approximately represented by cos(t) and cos(2t) where both harmonics have peaks in January and the second harmonic also has a peak in July. Petroleum demand is relatively constant throughout the year, so it is not included in this representation of the annual cycle of fossil-fuel carbon emissions. While different countries use different fuel mixes to supply their needs, the first harmonic is generally representative of heating demand

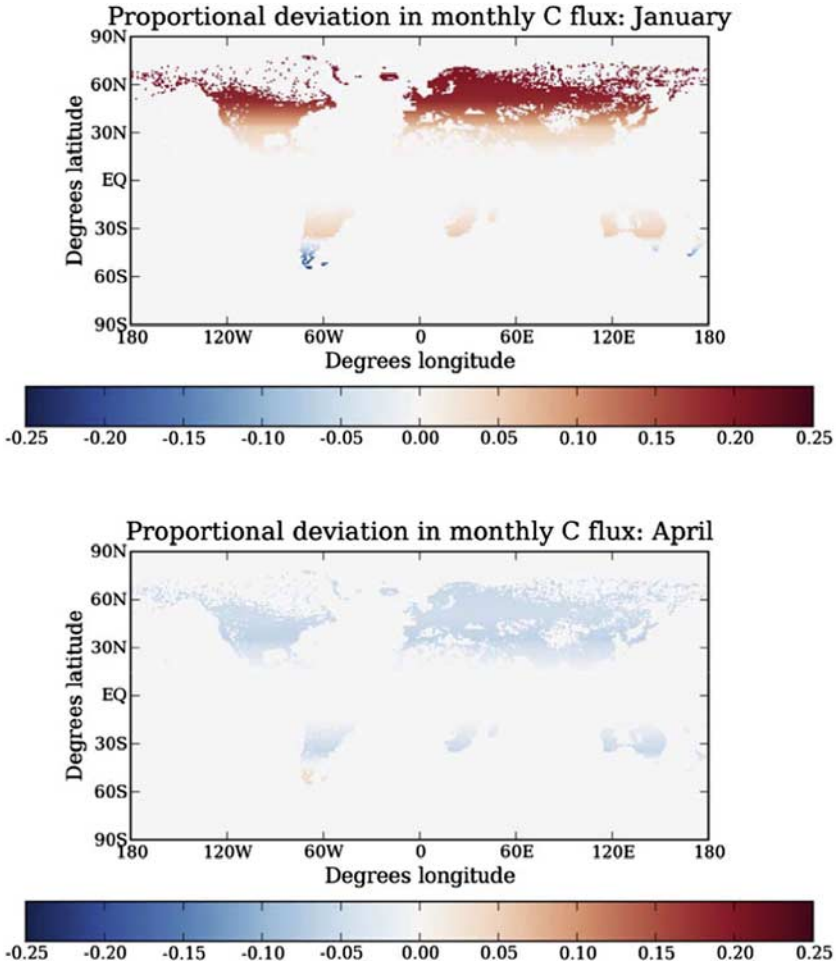

Figure 2. The estimated proportional deviations of monthly carbon flux from the annual mean for January, April, July and October. For a given grid cell, the color indicates the value of the calculated monthly flux divided by 1/12 of the annual flux. The red values show the increased fluxes relative to the annual mean that is a result of increased combustion in the winter months as described in section 2. The blue regions indicate where the carbon fluxes are lower than the annual mean.

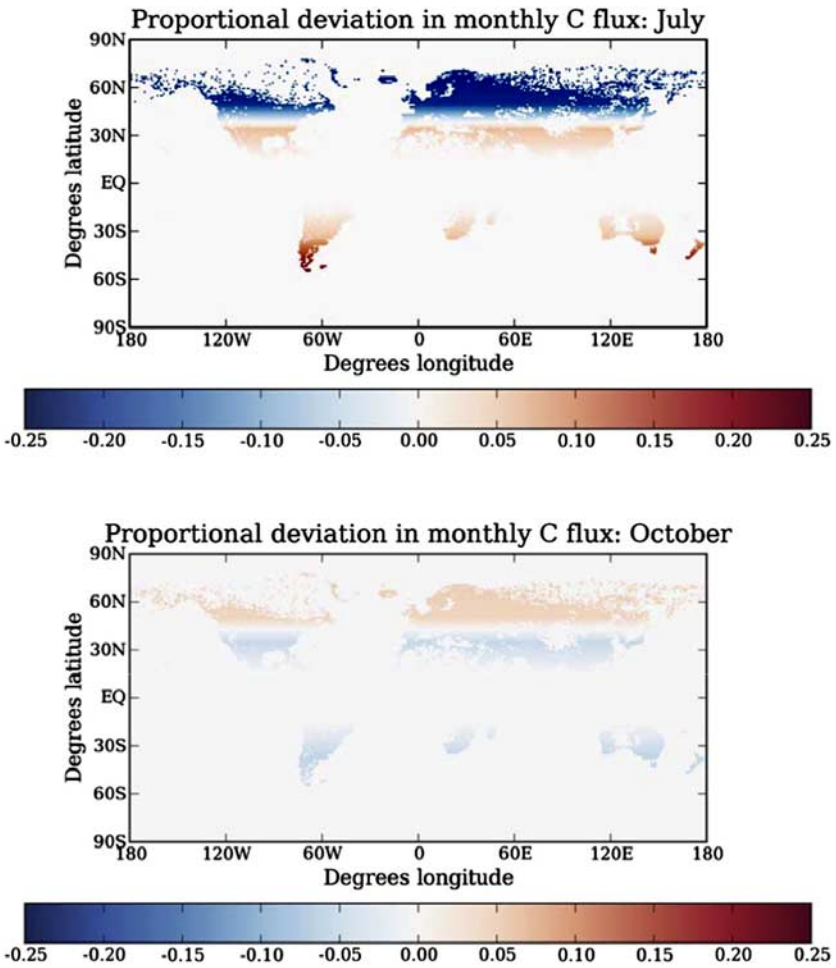

Figure 2. (continued)

and is the primary cause of month-to-month or season-to-season differences in carbon emissions at middle and high latitudes. A secondary summer peak in midlatitudes is seen where widespread availability of electricity makes it possible to air condition buildings. Based on these functions we have extrapolated to other countries based on the U.S. data. This is an important area where these calculations can be improved in the future.

[5] A heating function and a cooling function, representing carbon emissions from space comfort demands which vary appreciably and systematically over the course of a year, were superimposed on a base emissions function which is relatively constant from one season to the next. The base function represents transportation, industrial needs, residential and commercial needs such as water heating, food preparation, etc. The heating function is simplest at high latitudes (>50°) where it is represented by a simple cosine curve, peaking during the coldest months, regardless of the type of fuel used. The cooling function is closely related to electricity use in summer. Electricity use also peaks during winter due to some use of electricity for heating, and for lighting during the shorter winter days [*Blasing et al.*, 2005]. Between 15° and 35° the second harmonic was used to represent the seasonally changing carbon emissions related to electricity, including air-conditioning demands. In midlatitudes, between 35° and 50°, the winter peak of the 2nd harmonic is not sufficient to represent space comfort demands for heating, so a combination of the first harmonic (heating function) and the second harmonic was used in these latitudes as per the equations given below in section 2.1. In equatorial latitudes (0° to 15°), annual ranges of temperature and day length are relatively small, so no seasonal adjustments were used.

[6] The annual range of U.S. carbon emissions is around 15 Tg month-1 for natural gas and around 9 Tg month-1 for coal (Figure 1). This represents about 1 and 0.6 percent of annual U.S. fossil-fuel carbon emissions, which were around 1500 Tg for the period covered. Based on preliminary monthly data for a suite of states including Minnesota, Florida and others, we selected Fourier coefficients (described in section 2.1) to create annual ranges of first and second harmonics appropriate for each latitudinal section. These harmonics were then superimposed on a flat line representing annual totals [*Brenkert*, 1998], which in turn were based on population density data for 1990 [*Li*, 1996]. Scaling the amplitudes to annual totals helps to account for population-related variables, centers of industrial activity, and coastal moderation of climate, which reduces energy demand in winter and summer, thereby reducing the amplitudes of the harmonics used as well as total annual energy demand.

[7] In the tropics, annual ranges of temperature and day length are relatively small, so no seasonal adjustments were

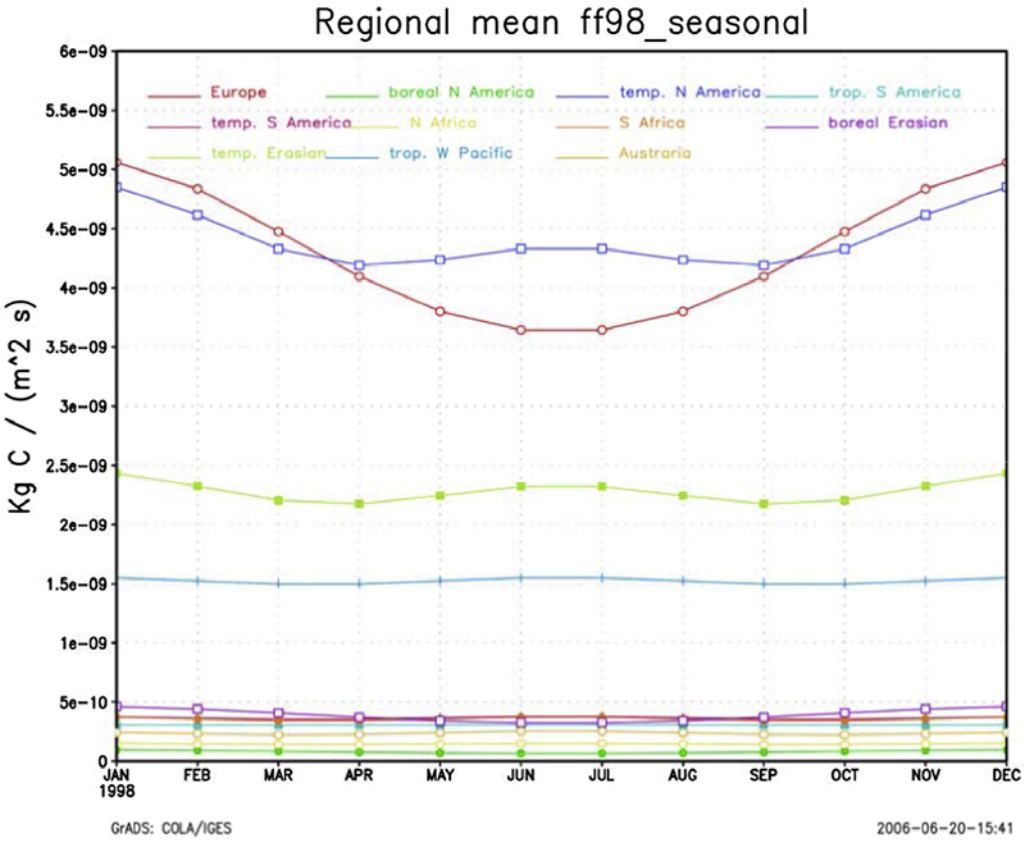

Figure 3. The anthropogenic CO_2 fluxes, in units of kg C m^{-2} s^{-1}, as a function of month for several geographic regions corresponding to the TransCom regions. These computations are derived from the anthropogenic fluxes for 1998. Clearly, the largest fluxes are in mid-high latitudes of the Northern Hemisphere.

used. North of 50 degrees, we assumed that air conditioning in summer was responsible for only a negligible percentage of fossil-fuel carbon emissions, and the amplitude of the 1st harmonic is simply proportional to the carbon emitted in any particular grid box. This may not be the case for some large cities north of 50 degrees, such as London or Berlin, but such refinements are left to further investigation of emissions at greater spatial resolution.

[8] In general, specification of the second harmonic is less accurate than the first because of heavy reliance on air conditioning in the United States, where monthly data were available for use in selecting the Fourier coefficients. Not all regions of the world have electricity, and many that do still lack the luxury of air conditioning. We have attempted to compensate for this problem by zeroing out the second harmonic in certain areas. Because carbon emissions from heating are also partially represented by the 2nd harmonic in latitudes 35–50, this approach detracts from the heating function in those latitudes. Moreover, places lacking electricity would also be expected to have a lower percentage of their carbon emissions from vehicle traffic, so the heating function would represent a larger percentage of the annual total from all functions. To adjust for these effects, the percentage range that would have been calculated and attributed to the second harmonic was added to that of the first harmonic in cases where the 2nd harmonic was, in fact, zeroed out.

2.1. Calculation of Estimated Monthly Carbon Flux

[9] We can formally describe the relationship between the annual carbon flux data and our estimated monthly carbon flux breakdown as follows: Dividing a year into 12 "months" each of 30 "days", at time t ∈ [0,360] the monthly carbon flux in Tg-C/month at a given grid cell with a non-zero annual flux is the annual total divided by 12 plus the corresponding value of one of the following functions:

$$\text{flux(t)} = (\text{Annual flux})/12 + 0.01 \cdot [A_1 \cdot \cos(t+\theta) + A_2 \cdot \cos(2t)]$$

where θ is a phase shift of 0° for northern latitudes and 180° for southern latitudes. The amplitudes A_1 and A_2 for the harmonics are determined by the degrees latitude (north or south) ϕ:

$$\phi \geq 50^\circ: \quad A_1 = [2 - 0.01*(90^\circ - \phi)]*(\text{Annual flux}); \quad A_2 = 0$$

$$35^\circ \leq \phi < 50^\circ: \quad A_1 = [1.6 - 0.1(50^\circ - \phi)]*(\text{Annual flux}) \quad A_2 = 0.04*(50^\circ - \phi)*(\text{Annual flux})$$

$$15^\circ \leq \phi < 35^\circ: \quad A_1 = 0 \quad A_2 = [0.6 - 0.03(35^\circ - \phi)]*(\text{Annual flux})$$

$$0^\circ \leq \phi < 15^\circ: \quad A_1 = 0 \quad A_2 = 0$$

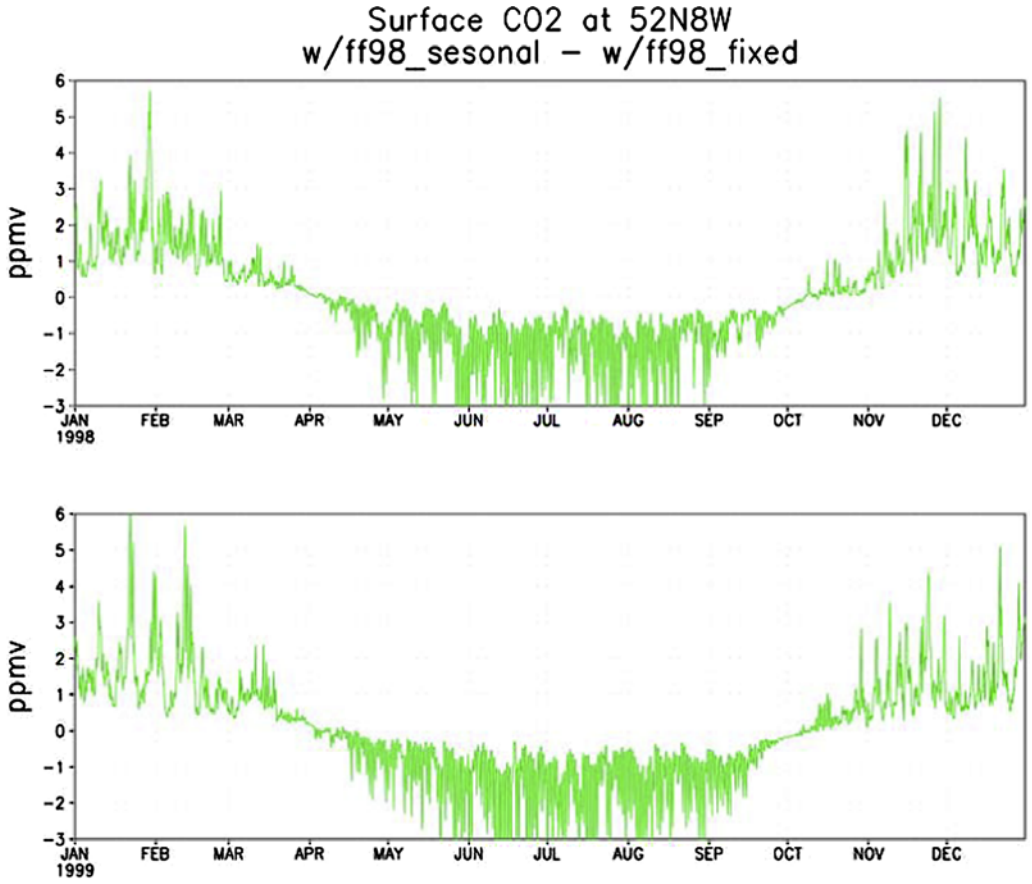

Figure 4. The difference between the hourly atmospheric CO_2 concentrations computed with a constant annual mean CO_2 flux and the monthly resolved fluxes computed for 1998 and 1999 for a location at 40N, 75W and at 52N, 8W. These sites were selected to investigate the impact on regions of two continents that are significantly impacted by anthropogenic CO_2 as well as the terrestrial biosphere. The upper panel shows the simulation for 1998, and the lower panel shows the simulation for 1999. Note that both the emissions and transport are specific for each year. Note the seasonality of the deviations from the general trend of concentrations. The mixing ratio difference is obtained by using the lowest model level that is 100 m deep.

To obtain the total emission for a grid cell for month i, we use a simple adaptive quadrature scheme from QUADPACK [*Piessens et al.*, 1983] to calculate

$$(\text{monthly total})_i = \frac{1}{30} \int_{(i-1)\cdot 30}^{i\cdot 30} flux(t)dt$$

To ensure correctness, the monthly totals for each cell are summed and checked for agreement with the annual flux data. Figure 2 shows the calculated flux departure from the annual mean for 4 example months. The results are discussed in section 3.

2.2. Test of Longitudinal Modifications to the Fluxes

[10] In a sensitivity test the monthly fluxes were generated using two harmonics with their amplitudes varying with latitude (section 2.1); however, the second harmonic was excluded in certain areas unless the grid square contained a large city, defined as having an annual anthropogenic CO_2 flux of more than 1 Tg C or a population over 1 million. In such large metropolitan areas, the effects of air conditioning might be non trivial. The areas for 2nd-harmonic exclusion were Central Asia (90–100 E, all latitudes; 80–110 E, N of 30 degrees), South America (40–80 W; 15–50 S), and Africa (10–40 E, 15–35 N and S). As the second harmonic was intended to represent lighting in the winter and air conditioning in the summer, this change would make the generated seasonality more accurate in areas unlikely to have electricity. These new seasonal fluxes are visibly somewhat different from the original ones, but the choice of emissions or population to determine exclusion seems to make little difference, as expected. We have not used these potential modifications in the transport simulations below. They made little difference because they were only applied to areas not likely to have electricity, and such areas emit relatively small amounts of CO_2. In any case, better estimates of the seasonal distribution of carbon emissions for many countries are expected soon.

3. Results

[11] Here we first discuss the monthly global gridded estimates of anthropogenic CO_2 flux derived from the

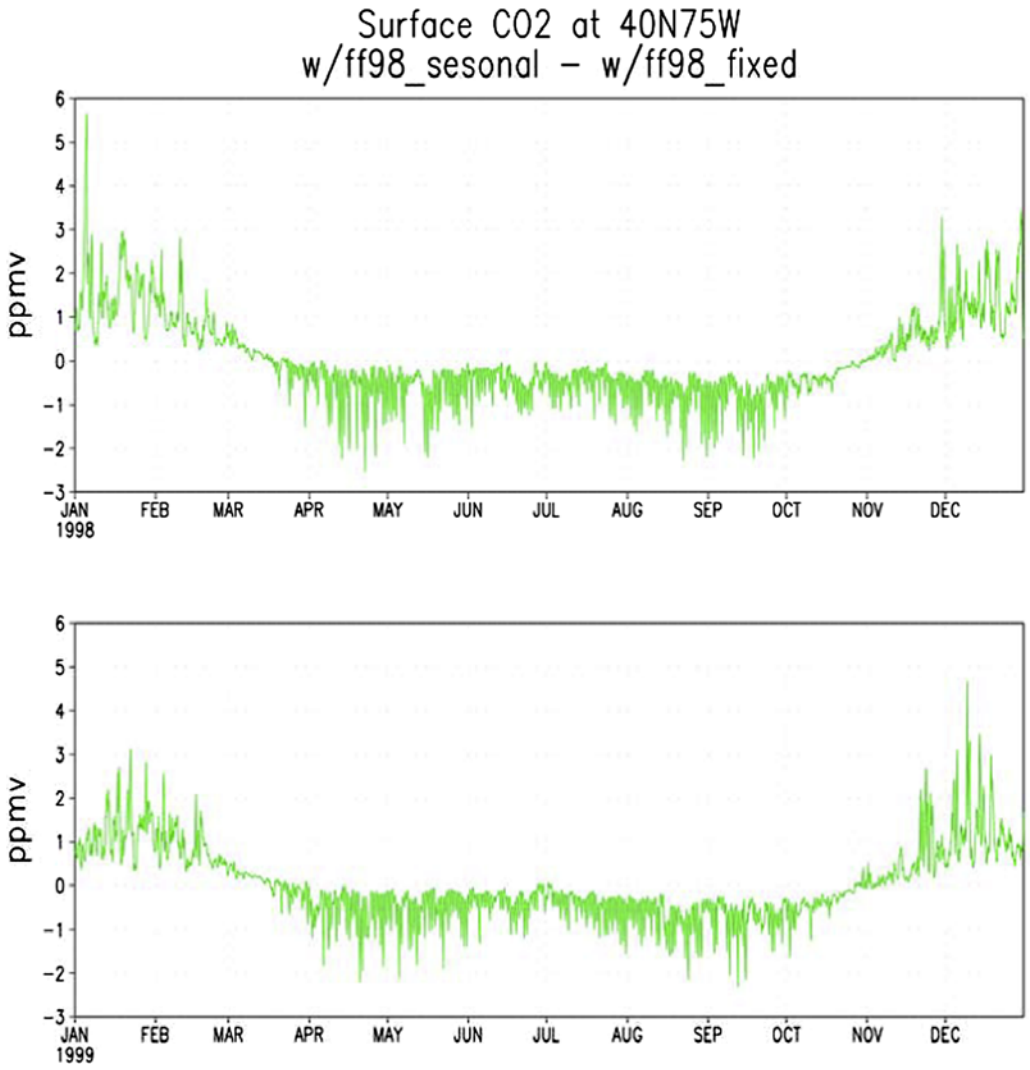

Figure 4. (continued)

method detailed in section 2.1. We then present an analysis of the impact these monthly surface CO_2 fluxes have on 3-D atmospheric CO_2 distributions via simulation in a global atmospheric transport model driven by assimilated meteorology [*Kawa et al.*, 2004]. These 3-D atmospheric CO_2 concentration estimates are then discussed in the context of inversion simulations of surface sources and sinks.

3.1. Monthly Anthropogenic Global CO_2 Fluxes: Latitudinal Analysis

[12] Figure 2 shows the proportional deviation of the CO_2 flux from the annual mean, for January, April, July and October. The red values show the increased fluxes relative to the base case (i.e., constant emissions) that resulted from increased combustion in the winter months; blue regions indicate fluxes below the base case. The figure illustrates that departures from the base case are greatest in winter at high latitudes and also significantly positive in summer at midlatitudes (near 30 N).

[13] Figure 3 shows the anthropogenic CO_2 fluxes, in units of kg-C m^{-2} s^{-1} as a function of month for several geographic regions as computed for 1998. Clearly, the largest fluxes are in mid-high latitudes of the Northern Hemisphere. These are also the regions with the largest seasonality as imposed by the chosen Fourier coefficients (section 2.1). The amplitude is largest in Europe because the relatively higher latitude imposes a lesser energy demand for air conditioning in summer. However, winter emissions in Europe are probably exaggerated because the amplitudes of the harmonics were fit to latitudes in North America, and winters in Europe are milder at the same latitudes. New estimates of monthly emissions for European countries will improve the accuracy of carbon transport estimates there. It is interesting to note that the impact of these monthly anthropogenic CO_2 fluxes are generally in phase with the fluxes due to the terrestrial biosphere. The highest anthropogenic fluxes are roughly at the same time as respiration in the terrestrial biosphere and lower when there is net CO_2 flux into the terrestrial biosphere due to photosynthesis.

3.2. Transport Calculations

[14] We have completed a suite of transport calculations, using the NASA Parameterized Chemistry and Transport Model (PCTM) with GEOS-4 meteorology [*Kawa et al.*, 2004; *Bloom et al.*, 2005], for CO_2 in the atmosphere using the monthly anthropogenic CO_2 fluxes described in previous sections. The GSFC Parameterized Chemistry and Transport Model (PCTM) is used for the CO_2 simulations

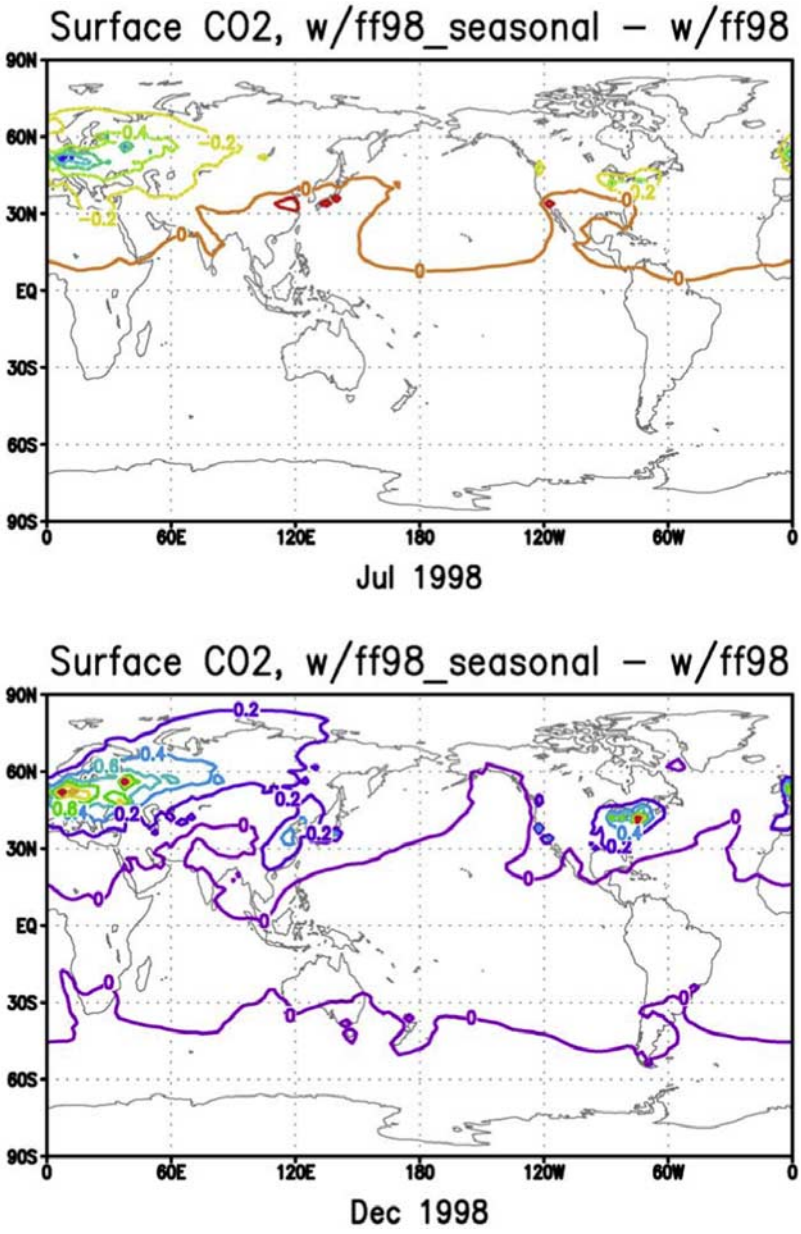

Figure 5. The global distribution of the July and December monthly mean CO_2 difference between concentrations computed with a constant annual mean CO_2 flux and the monthly resolved fluxes. The largest differences are located near the strongest sources of anthropogenic CO_2. The majority of the globe has differences below 1 ppmv. However, as the model resolutions get higher the ability to clearly identify sources and sinks will be impacted by these factors.

in this study. The CTM has been successfully used in a number of studies [*Strahan et al.*, 1998]. The advection is accomplished with a flux-form, semi-Lagrangian algorithm. The vertical transport due to subgrid processes of convection and turbulence vertical diffusion is computed with a semi-implicit scheme, using the diagnosed cloud mass flux and vertical diffusion coefficient from the GCM output of the fvDAS system.

[15] The model resolution is 2.5° in longitude and 2° in latitude. There are 25 unevenly spaced levels in the vertical, in which 14 are in the troposphere and 11 in the stratosphere. A hybrid sigma-pressure vertical coordinate is used as in the fvGCM. The wind, temperature, surface pressure data, as well as the diagnostic data of cloud mass flux and vertical diffusion coefficient, are from the assimilation system of fvDAS. The frequency of meteorological data input is 6 hours.

[16] Figure 4 shows the difference between the atmospheric CO_2 concentrations computed with an annual mean CO_2 flux and the monthly resolved fluxes computed as above for locations at 40N, 75W (New Jersey east of Philadelphia) and 52N, 8E (rural western Germany). These plots are from hourly saves of the transport model. These sites were selected to investigate the impact on regions of two continents that are significantly impacted by anthropogenic CO_2 as well as the terrestrial biosphere. The upper

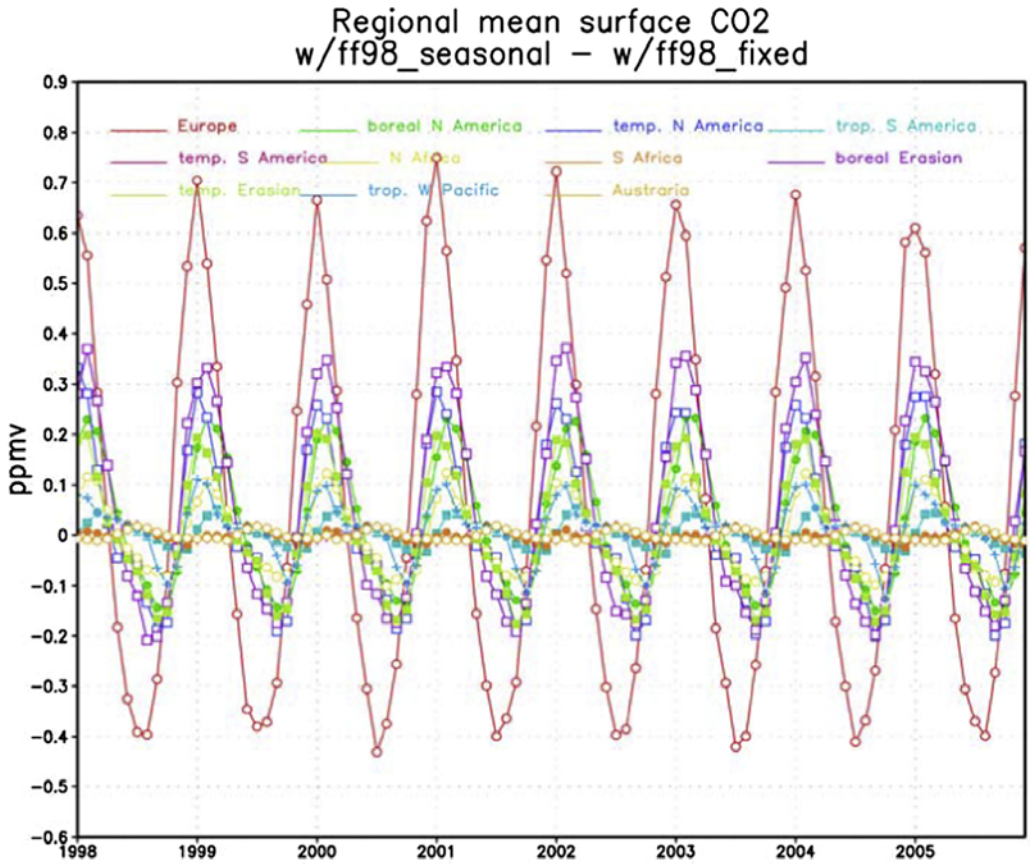

Figure 6. The regional mean surface level concentrations of atmospheric CO_2 over the 8-year period 1998–2005 as depicted as the difference between the annual mean and monthly CO_2 fluxes. On a regional basis the impact is 0.2–1.1 ppmv CO_2.

panel shows the simulation for 1998 and the lower panel shows the simulation for 1999. Note that both the emissions and transport are specific for each year. The plots show the difference between the constant annual mean fluxes and the monthly resolved fluxes. There is a significant impact on atmospheric CO_2 concentrations with differences of 1–6 ppmv in the seasonal cycle between the monthly flux run and the annual anthropogenic flux simulation. Note that near the sources, synoptic scale atmospheric circulations are important in the winter and that boundary layer venting and diurnal rectifier effects are more important in the summer. This is due to increased convection in summer. The large negative excursions in summer represent reduced CO_2 accumulation in the shallow nocturnal boundary layer. The positive, multi-day excursions in winter show the effect of synoptic systems with alternating stagnant and rapidly ventilated conditions and little diurnal variation of mixing depth. This affects the latitudinal gradient of near-surface CO_2 in the atmosphere; that annual, zonal mean gradient increases by about 0.05 ppmv when using the seasonally varying emissions [cf. *Gurney et al.*, 2005].

[17] Figure 5 shows the global distribution of the CO_2 difference for January and July. The largest differences are located near the strongest sources of anthropogenic CO_2. The majority of the globe has differences below 1 ppmv. In this simulation, fossil fuel CO_2 at the surface has a seasonal amplitude of 2 ppmv, that is nearly constant with latitudes north of the equator when using the seasonally varying emissions. The time-invariant fossil-fuel emissions also produce a seasonal cycle of 2 ppmv at the equator (owing to seasonal movement of the ITCZ), but the amplitude decreases to about 1.2 ppmv at high northern latitudes. Thus the seasonal fossil fuel emissions generate about 0.5 ppmv added amplitude in the seasonal cycle north of 30 N.

[18] Figure 6 shows the regionally averaged differences between simulated near-surface atmospheric CO_2 concentrations when fossil-fuel inputs were allowed to vary seasonally and when they were not, plotted for each month for the 8-year period 1998-2005. On a regional basis the impact on the seasonal amplitude is 0.2 – 1.1 ppmv CO2. Interannual CO_2 variability, created by variations in the meteorology, is small.

[19] Figure 7 shows the mean surface level concentrations of atmospheric CO_2 over the 8 year period 1998–2005 depicted as the difference between the annual mean and monthly CO_2 fluxes, for 3 observational sites: Park Falls, WI (LEF), Mauna Loa, HI (MLO), and the South Pole (SPO). The largest impact is at LEF with a seasonal cycle due to monthly anthropogenic CO_2 of 1.2 ppmv. Note that this site is far from most anthropogenic sources and is less impacted than the sites analyzed in Figure 4. This result is typical of moderately populated continental areas at mid-latitudes (see Figure 4). Little impact is seen at the remote sites in Figure 7.

[20] The ratio of local CO_2 concentrations to emissions can be useful in verifying modeled CO_2 emissions at small spatial scales. For example, *Pataki et al.* [2003] has shown a seasonal

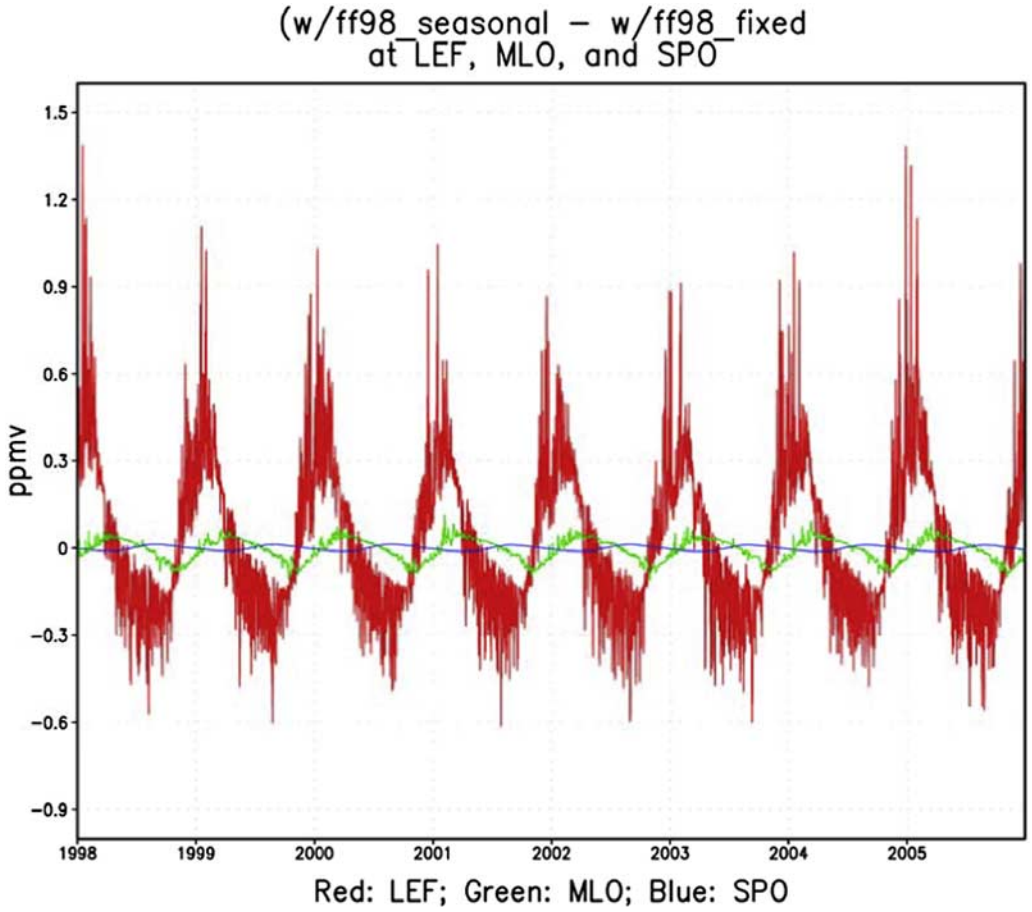

Figure 7. The mean surface level concentrations of atmospheric CO_2 over the 8-year period 1998–2005 as depicted as the difference between the annual mean and monthly CO_2 fluxes for three observational sites, LEF, MLO and SPO. The difference is largest at LEF with a seasonal cycle of 1.2 ppmv. Note that this site is far from most anthropogenic sources and is less impacted than the sites analyzed in Figure 4. For MLO, the model output from the level that includes the 600 mb level is used since the terrain is not resolved.

cycle in near-surface CO_2 concentrations over Salt Lake City, Utah (United States), which ranges from 500 parts per million by volume (ppmv) in winter to only slightly above global background levels (of 380 ppmv) in summer. Some of this is due to a decrease in local source strength in summer, when space-comfort needs are met by electricity generated at distant locations rather than by heat generated in local (e.g., residential) furnaces. A small amplitude may also be due to increased photosynthesis in summer. However, convection (or lack thereof in the stable wintertime Salt Lake valley) is an important influence on CO_2 mixing ratio accumulation at the CTM grid scale, and almost certainly so at local scales as well. It is expected that when the horizontal resolution of the PCTM starts to approach 10–50 km scales, these types of observed concentrations and ratios to local emissions will be better simulated.

4. Discussion and Conclusions

[21] There is significant seasonality in the anthropogenic flux of CO_2, and considerable geographical variation in that seasonality. A spatially variable 2-harmonic representation of the seasonal cycle is used to approximate these features. We then take these latitudinally dependent weighting factors and modify the constant annual CO_2 fluxes to reflect population and energy use to create the monthly anthropogenic CO_2 fluxes. We then implement the monthly CO_2 fluxes into a documented atmospheric transport model [*Kawa et al.*, 2004]. We find that there is significant, 1–6 ppmv, seasonal cycle of near-surface atmospheric CO_2 near and downwind of large emissions sources, due to the seasonal cycle of anthropogenic CO_2 alone.

[22] We also find that in the midlatitudes near the sources, synoptic-scale atmospheric circulations are important in the winter and that boundary layer growth and decay effects are more important in the summer. These findings have implications for inverse models that attempt to estimate surface source/sinks regionally especially when the surface sinks are colocated with regions of strong anthropogenic CO_2 emissions. Including the seasonality of fossil fuel emissions will lead to a diminished seasonality and interhemispheric gradient of the biospheric flux inferred from CO_2 observations. This result is an important conclusion of this study.

[23] It is clear that our estimation approach has shortcomings. It was noted above that fuel used for electricity will be a smaller percentage of the annual totals in large urban areas where carbon emitted from vehicle traffic is a larger percentage of the annual totals. However, this effect is partly compensated by the larger number of shopping malls

and other public places requiring air conditioning in summer and lighting during winter nights.

[24] Another shortcoming, characteristic of all other global CO_2 anthropogenic flux estimates, is the assumption that carbon emissions are distributed according to population density, which was an assumption inherent in annual totals obtained from *Brenkert* [1998]. Much electricity in the United States is generated at remote locations and used in more populated regions some distance away. Where generation and consumption occur in different regions, the use of population-weightings to geographically distribute carbon emissions mis-locates the carbon emitted from the generating facilities to the highly populated regions.

[25] In many cases, large cities within a country have electricity and air conditioning where rural regions do not. Better specification of the annual cycle of carbon emissions is needed on spatial scales finer than national averages provide. Many carbon-cycling processes take place at small time and space scales, and specification of carbon emissions at appropriate resolution is necessary for studies of such processes. In summer, photosynthesis reduces near-surface atmospheric CO_2 concentrations and convection dilutes them, while home heating, an important source of local CO_2 emissions, is relatively absent. This combination of increased sinks and decreased sources leads to near-baseline concentrations for much of the warm season. In winter, the reverse is true so that near-surface atmospheric CO_2 concentrations can accumulate to large values, especially in low-lying or geographically enclosed areas. For example, studies by *Pataki et al.* [2003] and *Henninger and Kuttler* [2004] have shown large increases in winter CO_2 concentrations in urban/industrial areas. Fossil-fuel carbon emissions, along with ecosystem respiration and suppression of convection are likely to be important. Efforts are underway to obtain more accurate estimates of carbon emissions for one-degree gridsquares [*Petron et al.*, 2006], but so far these have been confined to carbon from electricity generation in the United States. Finally, the monthly varying anthropogenic CO_2 fluxes are presently being used in inversion calculations, which will allow the impact of these fluxes on surface source-sink estimation to be assessed.

[26] **Acknowledgments.** D.E. acknowledges support from NASA grant NAG665462 to Duke University. D.E., Z.Z. and S.K. acknowledge support under NASA Carbon Cycle Science and the NASA High-End Computing Program. D.E., F.H., R.M., T.B., and M.D. acknowledge support from the U.S. Department of Energy, Office of Science and the Laboratory Directed Research and Development fund at Oak Ridge National Laboratory. Oak Ridge National Laboratory is managed by UT-Battelle, LLC, for the U.S. Department of Energy under contract DE-AC05-00OR22725. This research used resources of the National Center for Computational Sciences at Oak Ridge National Laboratory (ORNL). D.E. and F.H. acknowledge support from the Climate Change Research Division (CCRD) of the Office of Biological and Environmental Research (OBER), and by the Office of Advanced Scientific Computing Research (OASCR). J.G. acknowledges support from U.S. Department of Energy grant DE-FG02-03ER46030.

References

Andres, R. J., G. Marland, I. Fung, and E. Matthews (1996), Distribution of carbon dioxide emissions from fossil fuel consumption and cement manufacture, 1950–1990, *Global Biogeochem. Cycles*, *10*, 419–429.

Blasing, T. J., C. T. Broniak, and G. Marland (2005), The annual cycle of fossil-fuel carbon dioxide emissions in the United States, *Tellus, Ser. B*, *57*, 107–115.

Bloom, S., et al. (2005), The Goddard Earth Observation System Data Assimilation System, GEOS DAS Version 4.0.3: Documentation and validation, *NASA Tech. Memo., TM-2005-104606 V26,* 166 pp.

Bousquet, P., P. Peylin, P. Ciais, C. Le Quéré, P. Friedlingstein, and P. Tans (2000), Regional changes in carbon dioxide fluxes of land and oceans since 1980, *Science*, *290*, 1342–1346.

Brenkert, A. L. (1998), Carbon dioxide emission estimates from fossil-fuel burning, hydraulic cement production, and gas flaring for 1995 on a one degree grid cell basis, *NDP-058A,* Carbon Dioxide Inf. Anal. Cent., Oak Ridge Natl. Lab., Oak Ridge, Tenn. (Available at http://cdiac.ornl.gov/epubs/ndp/ndp058a/ndp058a.html)

Denning, A. S., I. Y. Fung, and D. A. Randall (1995), Latitudinal gradient of atmospheric CO2 due to seasonal exchange with land biota, *Nature*, *376*, 240–243.

Energy Information Administration (EIA) (2006), Monthly Energy Review, issued monthly, U.S. Dep. of Energy, Washington, D. C. (Available at http://www.eia.doe.gov/emeu/mer/contents.html)

Engelen, R. J., et al. (2002), On error estimation in atmospheric CO_2 inversions, *J. Geophys. Res.*, *107*(D22), 4635, doi:10.1029/2002JD002195.

Fan, S., M. Gloor, J. Mahlman, S. Pacala, J. Sarmiento, T. Takahashi, and P. Tans (1998), A large terrestrial carbon sink in North America implied by atmospheric and oceanic carbon dioxide data and models, *Science*, *282*, 442–446.

Gurney, K., et al. (2004), Transcom 3 inversion intercomparison: Model mean results for the estimation of seasonal carbon sources and sinks, *Global Biogeochem. Cycles*, *18*, GB1010, doi:10.1029/2003GB002111.

Gurney, K. R., Y. H. Chen, T. Maki, S. R. Kawa, A. Andrews, and Z. Zhu (2005), Sensitivity of atmospheric CO_2 inversions to seasonal and interannual variations in fossil fuel emissions, *J. Geophys. Res.*, *110*, D10308, doi:10.1029/2004JD005373.

Henninger, S., and W. Kuttler (2004), Mobile measurements of carbon dioxide within the urban canopy layer of Essen, Germany, paper presented at Fifth Conference on Urban Environment, Am. Meteorol. Soc., Vancouver, B. C., Canada, 23–26 Aug.

Kaminski, T., M. Heimann, and R. Giering (1999), A coarse grid three-dimensional global inverse model of the atmospheric transport: 2. Inversion of the transport of CO2 in the 1980s, *J. Geophys. Res.*, *104*(D15), 18,555–18,581.

Kawa, S. R., D. J. Erickson III, S. Pawson, and Z. Zhu (2004), Global CO_2 transport simulations using meteorological data from the NASA data assimilation system, *J. Geophys. Res.*, *109*, D18312, doi:10.1029/2004JD004554.

Li, Y.-F. (1996), Global population distribution 1990: Terrestrial area and country name information on a one by one degree grid cell basis, *ORNL/CDIAC-96, DB1016,* Carbon Dioxide Anal. Cent., Oak Ridge, Tenn. (Available at http://cdiac.ornl.gov/ndps/db1016.html)

Marland, G., and R. M. Rotty (1984), Carbon dioxide emissions from fossil fuels: a procedure for estimation and results for 1950–1982, *Tellus, Ser. B*, *36*, 232–261.

Marland, G., T. A. Boden, and R. J. Andres (2006), Global, regional, and national CO_2 emissions, in *Trends: A Compendium of Data on Global Change*, Carbon Dioxide Inf. Anal. Cent., Oak Ridge Natl. Lab., U.S. Dep. of Energy, Oak Ridge, Tenn.

Pataki, D., D. R. Bowling, and J. R. Ehleringer (2003), Seasonal cycle of carbon dioxide and its isotopic composition in an urban atmosphere: Anthropogenic and biogenic effects, *J. Geophys. Res.*, *108*(D23), 4735, doi:10.1029/2003JD003865.

Petron, G., et al. (2006), Moving towards improved fossil fuel emission inventories for the carbon cycle, in *Global Monitoring Annual Review*, *April 26–27*, p. 8, Earth Syst. Res. Lab., Boulder, Colo.

Piessens, R., E. de Doncker-Kapenga, C. W. Uberhuber, and D. K. Kahaner (1983), *QUADPACK: A Subroutine Package for Automatic Integration*, Springer, New York.

Randerson, J. T., M. V. Thompson, T. J. Conway, I. Y. Fung, and C. B. Field (1997), The contribution of terrestrial sources and sinks to trends in the seasonal cycle of atmospheric carbon dioxide, *Global Biogeochem. Cycles*, *11*, 535–560.

Strahan, S. E., A. R. Douglass, J. E. Nielsen, and K. A. Boering (1998), The CO2 seasonal cycle as a tracer of transport, *J. Geophys. Res.*, *103*(D12), 13,729–13,741.

U.S. Environmental Protection Agency (U.S. EPA) (2006), Inventory of U.S. greenhouse gas emissions and sinks: 1990–2004, Washington, D. C. (Available at http://www.epa.gov/climatechange/emissions/downloads06/06_Complete_Report.pdf)

R. J. Andres and T. J. Blasing, Environmental Sciences Division, Oak Ridge National Laboratory, Oak Ridge, TN 37831, USA.

M. Devries, D. J. Erickson III, F. M. Hoffman, and R. T. Mills, Computational Earth Sciences Group, Computer Science and Mathematics Division, Oak Ridge National Laboratory, Oak Ridge, TN 37831, USA.

J. Gregg, Geography Department, University of Maryland, College Park, MD 20742, USA.

S. R. Kawa and Z. Zhu, Laboratory for Atmospheres, NASA Goddard Space Flight Center, Greenbelt, MD 20771, USA.